engineering proceedings

MDPI

Proceeding Paper

Enhancing Indoor Position Estimation Accuracy: Integration of IMU, Raw Distance Data, and Extended Kalman Filter with Comparison to Vicon Motion Capture Data †

Tolga Bodrumlu [1,*] and Fikret Çalışkan [2]

[1] Istanbul Technical University
[2] Istanbul Technical University; caliskanf@itu.edu.tr
* Correspondence: bodrumlu@itu.edu.tr

† Presented at the 10th International Electronic Conference on Sensors and Applications (ECSA-10), 15–30 November 2023; Available online: https://ecsa-10.sciforum.net/.

Abstract: Indoor positioning systems are a significant area of research and development, helping people navigate within buildings where GPS signals are unavailable. These systems have diverse applications, including aiding navigation in places like shopping malls, airports, and hospitals, and improving emergency evacuation processes. The purpose of this study is to evaluate various technologies and algorithms used in indoor positioning. The study focuses on using raw distance data and Kalman filters to enhance indoor position accuracy. It employs a trilateration algorithm based on Recursive Least Squares (RLS) for initial position estimation and combines the results with accelerometer data. The designed algorithm using real sensor data collected in the ROS environment has been tested, and the results obtained are compared with data obtained from the Vicon Indoor Positioning System. In this comparison, the Root Mean Square Error metric is used. As a result of the comparison, it is observed that the error obtained from the designed algorithm is less than that of the Vicon system.

Keywords: indoor positioning; Extended Kalman Filter; ROS; sensor fusion

Citation: Bodrumlu, T.; Çalışkan, F. Enhancing Indoor Position Estimation Accuracy: Integration of IMU, Raw Distance Data, and Extended Kalman Filter with Comparison to Vicon Motion Capture Data. *Eng. Proc.* **2023**, *56*, x. https://doi.org/10.3390/xxxxx

Academic Editor(s): Name

Published: 15 November 2023

1. Introduction

In recent years, Unmanned Aerial Vehicles (UAVs) have found extensive applications in various fields, including military, industry, agriculture, as well as tasks like aerial photography and reconnaissance [1–3]. However, it's worth noting that these applications primarily take place outdoors and rely on robust GPS signals for accurate positioning. In cases where GPS signals are unavailable or weak, the precision of UAV positioning is significantly impacted. Presently, there is a growing need for indoor UAV technology, particularly for inspection purposes, which is closely tied to control optimization and precise path tracking.

Ultra-Wideband (UWB) technology has garnered significant attention due to its high precision in indoor positioning. UWB systems leverage short-duration pulses of radio waves spread across a wide spectrum, enabling accurate distance measurements through time-of-flight and trilateration techniques. Aiello and Shalom [4], delves into the principles of UWB and its significance in achieving precise and real-time positioning. Heimovirta, Salantera and Röning [5], discuss the practical implementation of a real-time indoor localization system based on UWB technology. This work focuses on the utilization of UWB for indoor positioning, providing insights into its application in real-world scenarios.

Vicon positioning systems are based on motion capture technology, utilizing cameras and markers to accurately track the movement and position of objects or individuals in a

controlled environment. Rhea [6], assesses the accuracy and precision of Vicon motion capture systems for tracking movements in three dimensions (3D). This work focuses on evaluating the reliability of Vicon systems in capturing 3D motion data. Gentil, de la Rouviere, and Elton [7], discuss Vicon as a computer vision solution for real-time 3D motion capture. It highlights the capabilities of Vicon technology in capturing and analyzing 3D motion data in real-time, particularly in the context of rehabilitation and neuroengineering. Benn and Martin [8], provide insights into the utilization of Vicon systems for capturing and analyzing motion data in the context of sports and healthcare.

In this paper, an accurate position estimation is calculated by combining the IMU and the raw distance data with the help of the Extended Kalman Filter (EKF). Initially, a position estimation is obtained using the Recursive Least Square (RLS) method with a trilateration algorithm. This solution, is used as a starting point for RLS. After, this position estimation is fused with the acceleration data. As a result, the estimated position obtained with the designed Extended Kalman Filter (EKF) is compared with the Vicon indoor positioning system, and the results are presented both graphically and in tabular form.

2. Position Estimation Algorithm

The position estimation algorithm is based on geometric approach and Extended Kalman Filter algorithms. After these algorithms are designed in a simulation environment, they are integrated into ROS (Robot Operating System) and tested with real sensor data, and the results are observed.

2.1. Geometric Approach

A geometric approach has been put forward in the basis of the study. As shown in the figure below, three reference points are given $B_1(x_1,y_1,z_1)$, $B_2(x_2,y_2,z_2)$ and $B_3(x_3,y_3,z_3)$ and d_1, d_2, d_3 interval measurements up to point A are given. The determination of the coordinates of the point A is carried out by solving the system of quadratic equations.

$$\begin{aligned}(x-x_1)^2+(y-y_1)^2+(z-z_1)^2 &= {d_1}^2\\ (x-x_2)^2+(y-y_2)^2+(z-z_2)^2 &= {d_2}^2\\ (x-x_3)^2+(y-y_3)^2+(z-z_3)^2 &= {d_3}^2\end{aligned} \quad (1)$$

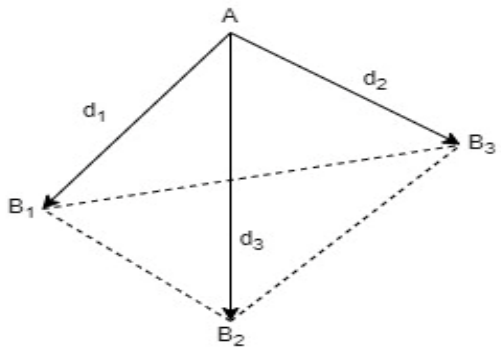

Figure 1. Reference Points and Interval Measurements.

The system of equations given here can be expressed as follows.

$$\begin{aligned}(x^2+y^2+z^2)-2x_1x-2y_1y-2z_1z &= {d_1}^2-x_1^2-y_1^2-z_1^2\\ (x^2+y^2+z^2)-2x_2x-2y_2y-2z_2z &= {d_2}^2-x_2^2-y_2^2-z_2^2\\ (x^2+y^2+z^2)-2x_3x-2y_3y-2z_3z &= {d_3}^2-x_3^2-y_3^2-z_3^2\end{aligned} \quad (2)$$

In addition to that, this expression can be shown in matrix form as below.

$$\begin{bmatrix} 1 & -2x_1 & -2y_1 & -2z_1 \\ 1 & -2x_2 & -2y_2 & -2z_2 \\ 1 & -2x_3 & -2y_3 & -2z_3 \end{bmatrix} \begin{bmatrix} x^2+y^2+z^2 \\ x \\ y \\ z \end{bmatrix} = \begin{bmatrix} s_1^2 - x_1^2 - y_1^2 - z_1^2 \\ s_2^2 - x_2^2 - y_2^2 - z_2^2 \\ s_3^2 - x_3^2 - y_3^2 - z_3^2 \end{bmatrix} \quad (3)$$

This matrix form generally can be expressed as follows.

$$A_0.x = b_0 \qquad x \in E$$
$$E = \{ (x_0, x_1, x_2, x_3)^T \epsilon \quad x_0 = x_1^2 + x_2^2 + x_3^2 \} \quad (4)$$

When examining the solution set, there are generally two different approaches. These are divided into three reference point-based and more than three reference point-based solutions. The details of these solution sets are elaborated in [9,10]. In brief, for the first scenario, the solution space varies depending on whether three reference points are in the same line or not. The second scenario involves having more than three reference points, which necessitates the use of the Recursive Least Squares method for the solution set.

Distance data is used together with the recursive least square algorithm to help to calculate the position. In the next section, the details of a more accurate position estimation with the help of EKF will be explained.

2.2. Sensor Fusion Algorithm

The systems's state vector is chosen as:

$$X = \begin{bmatrix} p(w) \\ v(w) \\ a(w) \end{bmatrix} \quad (5)$$

The vector p(w) denotes an object's position in the world coordinate system, specifying its coordinates on the x, y, and z axes as [px, py, pz]. The object's velocity along these axes in the world coordinate system is represented as v(w) = [vx, vy, vz] while its accelerometer data in the world coordinate system is denoted as a(w) = [ax, ay, az].

To elaborate further, the time interval between measurements is defined as Δt, and (Δt)w(k) defined as the process noise related to acceleration. Specifically, $\frac{\Delta t^2}{2} w(k)$ represents the process noise affecting velocity, and $\frac{\Delta t^3}{6} w(k)$ characterizes the process noise that influences position.

Equations of motion in the (k + 1) time interval can be expressed as follows:

$$p(k+1) = p(k) + v(k)(\Delta t) + a(k)\frac{\Delta t^2}{2} + \frac{\Delta t^3}{6} w(k)$$
$$v(k+1) = v(k) + a(k)(\Delta t) + \frac{\Delta t^2}{2} w(k) \quad (6)$$
$$a(k+1) = a(k) + (\Delta t) w(k)$$

The state equation can be represented in matrix form as follows:

$$x(k+1) = Ax(k) + Gw(k) \quad (7)$$

The matrices A and G, represent the transition matrix and noise process matrix respectively. Process noise vector and Q covariance can be defined as follows.

$$w(k) = [w_x(k)\ w_y(k)\ w_z(k)], Q = diag([\sigma_{ax}^2\ \sigma_{ay}^2\ \sigma_{az}^2])$$

$$A = \begin{bmatrix} 1 & 0 & 0 & \Delta t & 0 & 0 & \Delta t^2/2 & 0 & 0 \\ 0 & 1 & 0 & 0 & \Delta t & 1 & 0 & \Delta t^2/2 & 0 \\ 0 & 0 & 1 & 0 & 0 & \Delta t & 0 & 0 & \Delta t^2/2 \\ 0 & 0 & 0 & 1 & 0 & 0 & \Delta t & 0 & 0 \\ 0 & 0 & 0 & 0 & 1 & 0 & 0 & \Delta t & 0 \\ 0 & 0 & 0 & 0 & 0 & 1 & 0 & 0 & \Delta t \\ 0 & 0 & 0 & 0 & 0 & 0 & 1 & 0 & 0 \\ 0 & 0 & 0 & 0 & 0 & 0 & 0 & 1 & 0 \\ 0 & 0 & 0 & 0 & 0 & 0 & 0 & 0 & 1 \end{bmatrix}, G = \begin{bmatrix} \frac{\Delta t^3}{6} & 0 & 0 \\ 0 & \frac{\Delta t^3}{6} & 0 \\ 0 & 0 & \frac{\Delta t^3}{6} \\ \frac{\Delta t^2}{2} & 0 & 0 \\ 0 & \frac{\Delta t^2}{2} & 0 \\ 0 & 0 & \frac{\Delta t^2}{2} \\ \Delta t & 0 & 0 \\ 0 & \Delta t & 0 \\ 0 & 0 & \Delta t \end{bmatrix} \quad (8)$$

Observation vector $z(k)$ contains the distance values used in the geometric approach and an additional noise vector.

$$z(k) = \begin{bmatrix} d_1(k) + n_1(k) \\ d_2(k) + n_2(k) \\ d_3(k) + n_3(k) \\ d_4(k) + n_4(k) \end{bmatrix} = H(k)x(k) + n(k) \quad (9)$$

The observation matrix is represented by $H(k)$ and the vector of noise, with a mean of zero and a covariance matrix, is represented by $n(k)$.

$$R = diag([\sigma_{r1}^2\ \sigma_{r2}^2\ \sigma_{r3}^2\ \sigma_{r4}^2]) \quad (10)$$

where, r1, r2, r3, r4 are the distance values of the Marvelmind sensor to each other. The $H(k)$ observation matrix is a Jacobian matrix and is calculated as follows:

$$H(k) = \begin{bmatrix} \frac{\delta d_1(k)}{\delta p_x(k)} & \frac{\delta d_1(k)}{\delta p_x(k)} & \frac{\delta d_1(k)}{\delta p_x(k)} \\ \frac{\delta d_2(k)}{\delta p_x(k)} & \frac{\delta d_2(k)}{\delta p_x(k)} & \frac{\delta d_2(k)}{\delta p_x(k)} \\ \frac{\delta d_3(k)}{\delta p_x(k)} & \frac{\delta d_3(k)}{\delta p_y(k)} & \frac{\delta d_3(k)}{\delta p_z(k)} \\ \frac{\delta d_4(k)}{\delta p_x(k)} & \frac{\delta d_4(k)}{\delta p_x(k)} & \frac{\delta d_4(k)}{\delta p_x(k)} \end{bmatrix} \quad (11)$$

The equations described in the structure of the applied EKF are utilized. The initialization stage of this filter is one of the crucial factors, where the initial values of the covariance matrices are assigned. Subsequently, the prediction and update steps are executed in sequence.

$$\begin{aligned} \bar{\mathrm{x}}_\mathrm{k} &= \mathrm{f}(\hat{\mathrm{x}}_\mathrm{k}^{-1}, \mathrm{u}_\mathrm{k}) \\ \bar{\mathrm{P}}_\mathrm{k} &= \mathrm{A}_\mathrm{k}^{-1}\hat{\mathrm{P}}_\mathrm{k}^{-1}\mathrm{A}_\mathrm{k}^{-1\mathrm{T}} + \mathrm{Q}_\mathrm{k}^{-1} \\ K_k &= \bar{P}_k H_k^T [H_k \bar{P}_k H_k^T + R_k]^{-1} \\ \hat{\mathrm{x}}_\mathrm{k} &= \bar{\mathrm{x}}_\mathrm{k} + \mathrm{K}_\mathrm{k}\big(\mathrm{z}_\mathrm{k} - \mathrm{h}(\bar{\mathrm{x}}_\mathrm{k})\big) \\ \hat{P}_k &= (I - K_k H_k)\bar{P}_k \end{aligned} \quad (12)$$

In the following section, the integration of this geometric approach with EKF algorithms into the ROS platform will be described, and its implementation with real dataset will be discussed. The obtained results will be presented in detail.

3. Implementation and Simulation System Results

After the designed geometric approach and EKF structure, they are transferred to the simulation environment using C++. The code structure is integrated into the PX4 code, making it compatible with the ROS environment. The acceleration data from UWB sensors is received at approximately 40 Hz, while the raw distance data arrives at around 80 Hz. To address this discrepancy, time synchronization is achieved between the acceleration and distance data. The acceleration data is upsampled to 80 Hz using interpolation. Additionally, since Vicon data is received at a rate of 20 Hz, it is necessary to perform time synchronization with the position data obtained from EKF results. Therefore, Vicon data is upsampled to 80 Hz using interpolation to ensure proper time synchronization.

When looking at Figures 2 and 3, it is easily noticeable that the X, Y, and Z positions obtained from the EKF are closer to the reference results than those obtained from the Vicon system. Additionally, Figure 3 depicts the differences between the EKF and Vicon in relation to their respective reference values. Examining the position error values in Table 1, it is observed that the average difference between the EKF and the reference is 0.205 m, while for the Vicon, this difference is 0.255 m. Moreover, when looking at the minimum and maximum errors, it is evident that the values obtained from the EKF are lower than those obtained from the Vicon system. In summary, through a numerical comparison of the results, it is apparent that the designed EKF algorithm provides better results compared to the Vicon positioning system.

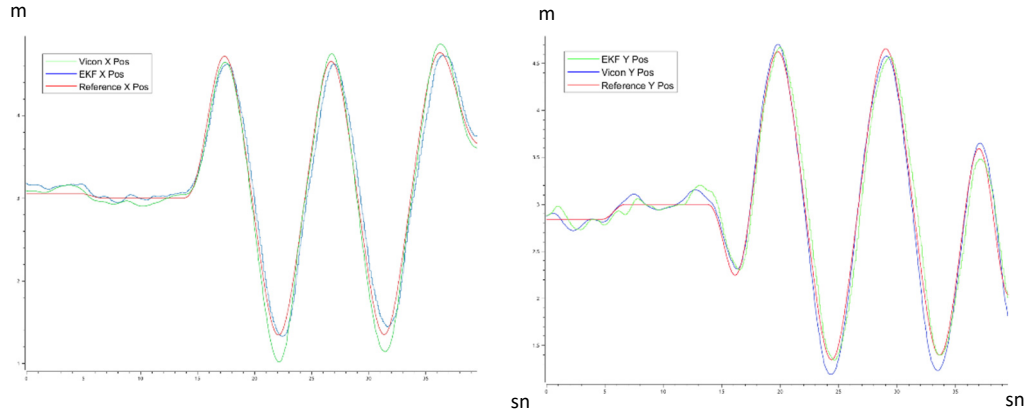

Figure 2. X and Y positions (Vicon-EKF-Reference).

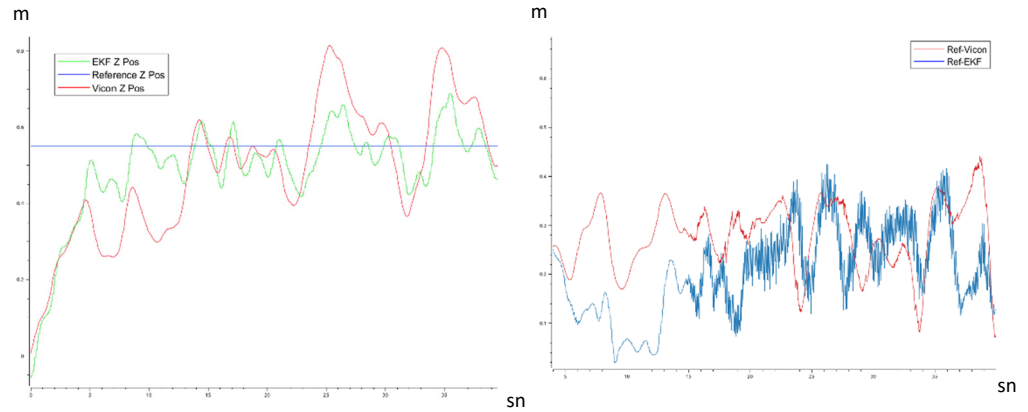

Figure 3. Z position and Vicon and EKF differences from reference.

Table 1. Position Error Values.

	Minimum Error (m)	Mean Error (m)	Maximum Error (m)
Ref-EKF	**0.019**	**0.205**	**0.424**
Ref-Vicon	**0.07**	**0.255**	**0.441**

4. Conclusions

In this study, position estimation is calculated by fusing raw distance data with the IMU using sensor fusion algorithms, specifically through the Extended Kalman Filter. The fundamental structure of the designed algorithm incorporates a geometric approach. Firstly, a position calculation is derived from the geometric approach, and then the accuracy of this position is enhanced using an accelerometer data and the EKF algorithm. The designed algorithm is transformed into the C++ environment and integrated into ROS (Robot Operating System). Real sensor data is used during the testing of the algorithm. Sensor data is collected using the ROS platform, and the algorithm is executed within ROS to observe the obtained results. According to the results obtained, the designed EKF structure yielded more successful outcomes compared to the Vicon position system. These results are supported both graphically and through numerical tables.

Funding: This research was partially financially supported by Istanbul Technical University, grant number 42754.

Institutional Review Board Statement: Not applicable.

Informed Consent Statement: Not applicable.

Data Availability Statement: Not applicable.

Conflicts of Interest: The authors declare no conflict of interest.

References

1. Valavanis, K.P.; Vachtsevanos, G.J. *UAV Applications: Introduction*; Springer: Amsterdam, The Netherlands, 2015.
2. Samad, T.; Bay, J.S.; Godbole, D. Network-centric systems for military operations in urban Terrain: The role of UAVs. *Proc. IEEE* **2007**, *95*, 92–107.
3. Li, Z.; Liu, Y.; Walker, R.; Hayward, R.; Zhang, J. Towards automatic power line detection for a UAV surveillance system using pulse coupled neural filter and an improved Hough transform. *Mach. Vis. Appl.* **2010**, *21*, 677–686.
4. Aiello, R.; Bar-Shalom, Y. Ultra-Wideband Technology for Precise Real-Time Location Systems. *Proc. IEEE* **2000**, *88*, 62–85.
5. Heimovirta, E.; Salantera, S.; Röning, J. Real-Time Indoor Localization Using Ultra-Wideband Technology. In Proceedings of the 11th International Conference on Mobile and Ubiquitous Systems: Computing, Networking and Services, London, UK, 2–5 December 2014; pp. 265–274.
6. Rhea, C.K. Accuracy and Precision of Vicon Motion Capture Systems for Tracking in 3D. *Gait Posture* **2004**, *20*, 332–335.
7. Gentil, C.; de la Rouviere, S.; Elton, C. Vicon: A Computer Vision Solution for Reliable Real-Time 3D Motion Capture. *J. NeuroEng. Rehabil.* **2009**, *6*, 11.
8. Benn, A.; Martin, A. Vicon Revue: Motion Capture Technology for Rehabilitation and Sports Medicine. *Biomech. Med. Swim.* **2004**, *IX*, 122–126.
9. Norrdine, A. An Algebraic Solution to the Multilateration Problem. In Proceedings of the 2012 International Conference on Indoor Positioning and Indoor Navigation, Sydney, Australia, 13–15 November 2012; pp. 1–4.
10. Bodrumlu, T.; Caliskan, F. Indoor Position Estimation Using Ultrasonic Beacon Sensors and Extended Kalman Filter. *Eng. Proc.* **2022**, *27*, 16. https://doi.org/10.3390/ecsa-9-13353.